

Superhydrophobic and Low Reflectance Carbon Nanotubes Buckypapers

Rodrigo Bezerra Vasconcelos Campos^{a*} , Tiago Damasceno da Rocha^a, Mauro Meliga Wysard Jr.^b,

Sergio Alvaro de Souza Camargo Jr.^{a,b}

^aUniversidade Federal do Rio de Janeiro, COPPE, Programa de Engenharia da Nanotecnologia, Av. Horácio Macedo 2030, Centro de Tecnologia, Bloco G, Sala 103-A, Cidade Universitária, 21941-972, Rio de Janeiro, RJ, Brasil.

^bUniversidade Federal do Rio de Janeiro, COPPE, Programa de Engenharia Metalúrgica e de Materiais, Av. Horácio Macedo 2030, Centro de Tecnologia, Bloco F, Sala F-214, Cidade Universitária, 21941-598, Rio de Janeiro, RJ, Brasil.

Received: March 17, 2022; Revised: July 18, 2022; Accepted: August 30, 2022

In this paper, carbon nanotube (CNT) buckypapers (BPs) were produced by vacuum filtration of CNT water suspensions prepared by sonication using 0.5 wt % of Triton X-100 dispersing agent. The as-produced BPs were efficiently dispersed and presented very low optical reflectance, with an average reflectance of 1.30% in the visible range and hydrophilic/oleophilic properties, readily absorbing water or oil liquid drops through their network of pores. Plasma treatment with 1, 1, 1, 2 tetrafluoroethane (C₂H₂F₄) turned the BPs superhydrophobic with water contact angles (CA) greater than 140°, while still maintaining their oleophilic properties unchanged. This effect is attributed to the combination of the decrease of surface energy and modification of the surface structure with micro/nanopores due to the coating with a fluorocarbon film. After only 1 minute plasma treatment, the BPs presented high hydrophobicity (CA = 145°) while keeping their oleophilicity and the very low optical reflectance essentially unaffected. These results indicate that a good combination of low reflectance and a superhydrophobic/oleophilic behavior can be achieved which is of importance for technological applications that require super black surfaces and prevent water from being absorbed, improving the handling of optical signals and increasing the useful life of materials.

Keywords: Carbon nanotubes, buckypaper, superhydrophobic, surface treatment, reflectance.

1. Introduction

The ability of a surface to repel or adhere/absorb liquids, such as water or oil, has an extremely important impact on its applications, such as obtaining self-cleaning, antifouling and anti-icing properties. The modification of surface properties of materials can be achieved through several techniques, including plasma-enhanced chemical vapor deposition (PECVD), plasma electrolytic oxidation (PEO), sputtering, and laser ablation. The latter is also a prominent technique used to obtain black coatings involving the oxidation of metallic substrates (Al, Mn, Ti or Zr) in aqueous electrolyte solutions¹. Black coatings can also be obtained using carbon nanotubes (CNTs), reaching reflectance values lower than 1% in the case of Vantablack², or as thin films deposited onto surfaces by spray coating or used in the form of freestanding sheets, known as buckypapers (BPs)³. Vantablack consists of a set of aligned carbon nanotubes (hence the prefix VANTA - Vertically Aligned NanoTube Arrays) grown by chemical vapor deposition, that is capable of absorbing 99.965% of light (750 nm wavelength)². The preparation of CNT coatings is much cheaper and simpler than other coating techniques, scalable and can be adapted to irregular-shaped objects or substrates. Surface treatment

is a process that modifies a given surface by improving or adding properties. Treating a surface with plasma creates a long-lasting nano-scale layer that uniformly covers a surface within minutes in a non-destructive process. It can confer water or oil phobicity/phobicity properties that can be used in solar power applications, reduction of stray light in optical systems, and self-cleaning systems³⁻⁶.

One method of altering the morphology of CNT is through covalent functionalization, which can be divided into direct sidewall and defect group functionalization. Fluoride functionalization of CNTs occurs through direct sidewall functionalization, where F is attached on the sp² network, altering the hybridization of a sidewall carbon atom to sp³ and, therefore, forming a covalent bond with it⁷. When not functionalized, these orbitals (pi electrons) interact with visible light, giving the appearance of black color. Once functionalized, these free pi-orbitals cease to exist, causing an increase in reflectance⁸. Therefore, a PECVD treatment of a CNT-coated surface results in a superhydrophobic low-reflectance surface.

Carbon nanotubes are a very versatile material due to their morphology, and since their discovery in 1991 by Iijima⁹, remarkable progress has been made in many different applications^{8,10-15}. The term “buckypaper” was coined in

*e-mail: vasconcelos@coppe.ufrj.br

2003 by Richard Smalley and his research group. BP is a dispersed matrix of carbon nanotubes held by Van der Waals interactions¹⁶. They can be produced using single-walled (SWCNT), double-walled (DWCNT) and multi-walled carbon nanotubes (MWCNT). BP can be prepared by dispersing the CNTs and a dispersing agent in a solvent followed by a sonication using a probe sonicator. Although the CNTs are not soluble in water, the high energy of the sonicator allows the agglomerations of nanotubes to be physically separated^{17,18}. Thus, it is possible to obtain individual and stable nanotubes in the suspension through the non-covalent interactions with the dispersing molecules. After the dispersion, the nanotube suspension is forced through a microporous membrane using vacuum filtration or positive pressure, resulting in a freestanding paper-like structure with an anisotropic morphology.

However, in order to the produced buckypaper to be able to fully extract the benefits of using carbon nanotubes, they must be efficiently dispersed in an adequate solvent. Some studies showed that the bundles and clusters of nanotubes result in a decrease in the properties of the composites compared to theoretical studies based on individual carbon nanotubes¹⁹⁻²². Therefore, one of the main challenges has been the incorporation of individual carbon nanotubes or at least relatively small clusters of nanotubes within the array of other materials^{19,23}.

Surfactants are one of the most known and efficient types of materials to aid the dispersion of nanoparticles in a solution. Surfactants are amphiphilic molecules, which can easily interact with polar and nonpolar systems. Therefore, surfactants are extremely attractive to the dispersion of carbon nanotubes in a selected solvent. Of the important characteristics that a surfactant must have to be an effective dispersing agent of nanotubes the presence of fillers, the size of the hydrophobic region and the presence of aromatic groups are among the most important ones²⁴⁻²⁶.

Tan et al.²⁷ established criteria to evaluate the degree of dispersion of nanotubes using different concentrations of surfactants. Among the surfactants used, the non-ionic surfactant Triton X-100 presented excellent results by forming a large layer of solvation of the hydrophilic parts of the surfactant around the nanotubes²⁸⁻³⁰. The molecules of surfactant propagate between the spaces formed between the clusters of carbon nanotubes due to the shear stresses generated during the sonication process to separate the carbon nanotubes. Strano et al.³¹ explained this phenomenon as a gradual exfoliation process when dealing with single-walled carbon nanotubes and designates an unzipping effect when it is multi-walled nanotubes. By means of the spaces generated by the ultrasound, the molecules of surfactant adsorb on the surface of the carbon nanotubes, preventing them to agglomerate again.

The definition of wettability refers to the extent the interface between two compounds interacts with each other, so if a solid material has an affinity to a liquid, a spontaneous interfacial area expansion will occur. Thus, in the case of a solid/liquid interaction wettability is a factor dependent on the chemical composition of the involved compounds and the solid surface roughness. In order to obtain an oleophilic/hydrophobic material, it is necessary

to employ a coating with surface energy smaller than the surface tension of water (72 mN/m), but higher than that of oil (20-30 mN/m)³². Fluorocarbon films have low polar and high nonpolar characteristics due to the CF_x groups in their molecular structure, resulting in a low surface energy material. Therefore, when applied to a porous substrate, it is expected that such a coating will allow the oil to pass through the pores and block the passage of water, separating water from oil. In addition, its water repellency suggests its use in self-cleaning and icephobic applications³³.

Oleophobic surfaces also tend to repel water. This is because water has a higher surface tension than oil. The literature reports the obtaining of these types of surfaces by using tensioactive fluorides (or surfactant fluorine)³³⁻³⁵. The process in which the drop of water is repelled is known as “non-flip-flop” and when water penetration occurs, it is called “flip-flop”. However, many current examples of “flip-flop” processes present several disadvantages, including poor oleophobicity or low water penetration³⁵.

In this study, multi-walled carbon nanotubes buckypapers were produced, submitted to plasma treatment using tetrafluoroethane and characterized to obtain a low reflectance and superhydrophobic material.

2. Experimental

2.1. Preparation of buckypapers

A probe sonicator was used to assist the dispersion of nanotubes. Dispersions of MWCNTs (150 mg) were sonicated in an aqueous solutions (100 ml) of 0.5% Triton-X 100 ($\text{C}_{14}\text{H}_{22}\text{O}(\text{C}_2\text{H}_4\text{O})_n$) for different sonication energies. The dispersions were sonicated at a frequency of 20 kHz using pulses of 2.0 seconds with intervals of 2.0 seconds to avoid overheating the solution. To identify the influence of the dispersion energy of the nanotubes in water, the samples were sonicated with energies ranging from 500 to 15,000 J. The carbon nanotubes used were supplied by CTNano/UFGM. These are MWCNTs with a purity greater than 95%, tube length ranging from 5 to 30 μm and diameter dispersion ranging from 10 to 50 nm.

To prepare the BPs, a vacuum filtration system was used to percolate the suspension containing CNTs through a PTFE microporous membrane (Millipore, pore size 0.45 μm) resulting in a homogeneous final product as shown in Figure 1. The microporous structure of the membrane allows water to pass through it, retaining the carbon nanotubes. While still adhered to the membrane, the sample was rinsed with deionized water for six cycles. Each cycle consists of rinsing the sample with 100 ml of deionized water to remove residues of Triton X-100. As reported by several studies, this is an effective method for the removal of Triton X-100^{29,36-38}. The BP was then kept at room temperature for 2 hours to dry and, finally, it was placed in an oven at 100 °C for 12 hours to remove any residual solution. After drying, the BP was detached from the membrane with plastic tweezers.

2.2. Plasma treatment

The fluorocarbon films were deposited onto (100) crystalline silicon and BPs using a commercial fluorocarbon gas as a

precursor (1,1,1,2-tetrafluoroethane, $C_2H_2F_4$, R-134A, Chemours, purity 98.5%), in a plasma-enhanced chemical vapor deposition (PECVD) system, consisting of a conventional parallel plate capacitively coupled glow discharge reactor (radio-frequency; 13.56 MHz) commonly employed to deposit amorphous carbon-related materials. The samples were placed on the circular anode of the system, which is 2.5 cm apart from the cathode, both with an area of 50 cm^2 . Figure 2 shows the schematics of the RF-PECVD system in which the buckypapers were submitted to plasma treatment for three different treatment times (1, 3 and 10 minutes). A base pressure below 1.0×10^{-3} Pa was attained in the chamber before deposition. During the deposition, the gas pressure and flow were kept constant at 10 Pa and 15 sccm, respectively. First, films were deposited on silicon substrates with different rf powers applied to the cathode from 5 W to 50 W. After the evaluation of the films by contact angle measurements, the deposition parameters of the best performance were chosen to coat the BPs.

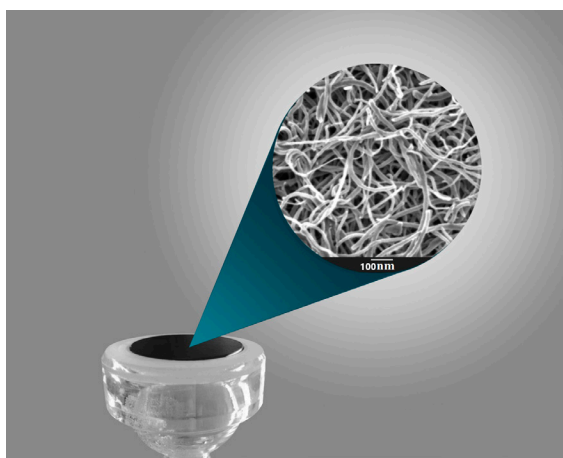


Figure 1. Buckypaper (BP) supported by a microporous membrane after vacuum filtration.

2.3. Characterization

Diffuse reflectance measurements were carried out in the range of the visible light (400 to 700 nm) at a scan rate of 30 nm/min using a spectrophotometer Evolution 300 (Thermo Scientific). The reflectance values were calibrated against a sapphire sample. Fluorocarbon films deposited on silicon substrates under the same deposition conditions were characterized by Fourier transform infrared absorption spectrometry (FTIR, Spectrum 100, Perkin Elmer). Each spectrum was obtained from 256 scans in the range of $500 - 4000\text{ cm}^{-1}$ with a resolution of 4 cm^{-1} . X-ray photoelectron spectroscopy (XPS) was performed in an ESCA Plus System (Omicron Nanotechnology) in ultra-high vacuum using an Mg X-ray source ($K\alpha = 1,253.6\text{ eV}$), with an emission current of 16 mA and voltage of 12.5 kV with 80 degrees take-off angle. The high-resolution spectra were obtained at 0.05 eV steps. The spectra were calibrated using a pure graphite sample (Nacional de Grafite) with a bonding energy of 284.6 eV.

To determine the BPs wettability, contact angle measurements were carried out using the sessile drop method in an optical contact angle measuring apparatus (OCA-20, Ramé-Hart). Three water drops with a volume of $5\text{ }\mu\text{L}$ were deposited on the surface of each sample and for each drop, 50 values of contact angle were measured from both sides of the drop and the obtained result is the average of all measurements. Following the same procedure, measurements of contact angle with the mineral oil Nujol® (Schering-Plough S.A.) were conducted to assess the oleophobicity/oleophilicity of the buckypapers.

3. Results and Discussion

Dispersions with and without the use of surfactant were prepared according to the procedure described in section 2.1, and the degree of dispersion was assessed by photographic records 30 minutes after being sonicated. In the first group

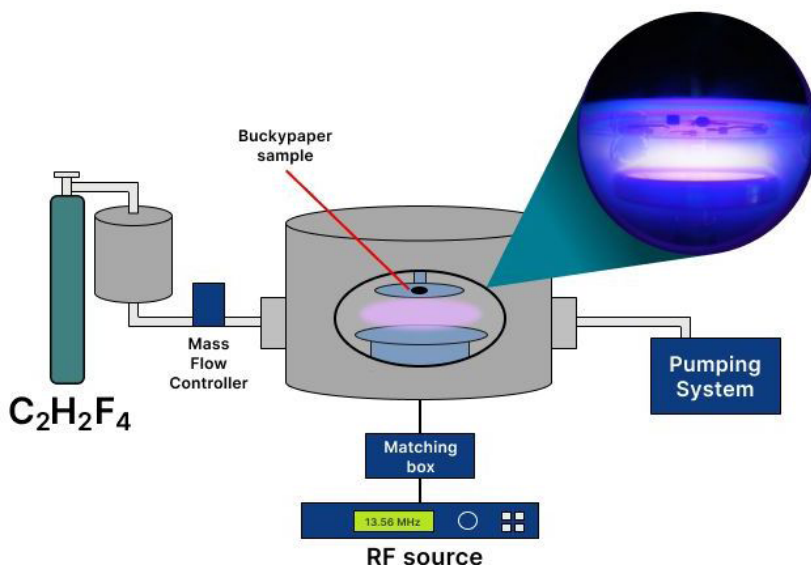


Figure 2. Schematic representation of the RF-PECVD system used for the plasma treatment of buckypapers and a detail picture of the plasma.

of samples, shown in Figure 3a, which was prepared without the use of surfactant, none of the samples presented a stable dispersion. Because of the van der Waals force, which governs the nanotube interactions, agglomerations started to form minutes after sonication. All samples from this group showed the same behavior. This experiment was crucial in determining the importance of the surfactant in the dispersion.

On the other hand, Figure 3b shows the increasing degree of dispersion of the group of samples prepared with the addition of surfactant. As one can observe, there are no visual differences between the samples prepared with different sonication energies. The use of surfactant accounts for this behavior, which is attributed to “the unzipping effect”³⁹. During the ultrasonic dispersion process, the agglomerations of carbon nanotubes break due to the impact of longitudinal waves (compression and decompression zones). A gradual exfoliation process happens to a point where the surfactant molecules interact and adhere to individual nanotubes preventing them from re-agglomerate.

The effect of sonicator energy on the suspensions prepared with surfactant is shown in Figure 4. Figure 4a shows the UV-Vis absorption spectra of the MWCNT dispersions prepared with 0.5 wt. % of Triton X-100 surfactant obtained with different sonication energies. It is known that isolated CNTs present strong UV absorption associated with an electronic transition related to the p plasmon. This transition is suppressed by nanotube agglomeration. Therefore, a measurement of the UV absorbance of CNT suspensions can be used as a measure of the dispersion of the suspensions^{40,41}. As seen in Figure 4, the UV absorbance of the suspensions prepared with surfactant increases steadily as the sonication energy is increased from 500 J to 13,000 J, suggesting a continuously increasing dispersion.

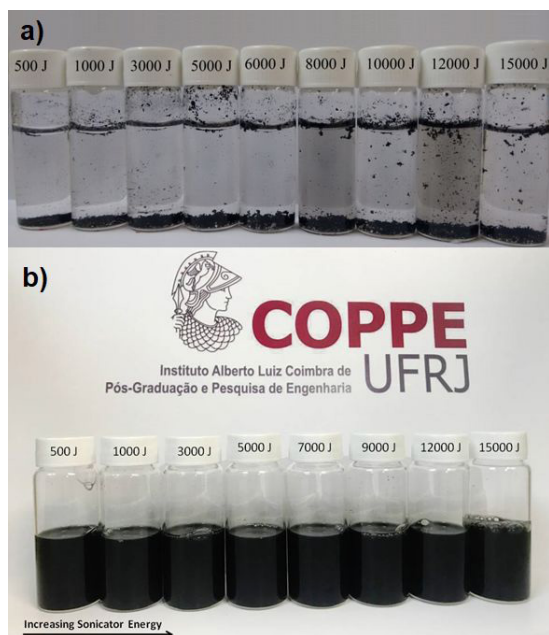


Figure 3. Photographic record of MWCNT dispersions in water 30 min after sonication with different energies: without (a) and with (b) the use of 0.5 wt.% of Triton X-100 surfactant.

The exfoliation of the nanotubes (unzipping) is potentialized by the electrostatic forces generated among the surface charges of the CNTs and the Triton X-100. Therefore, it is possible to assess the dispersion stability through the zeta potential of the suspensions. Generally, a zeta potential out of the ± 25 mV range indicates a stable dispersion. In other words, coagulation of solid particles in the suspension is unlikely when the zeta potential is out of this range because of the surface charges present on the solid particles. As for the assessment of suspensions by means of Zeta potential, it is possible to state from Figure 4b that the samples sonicated with energies of 3000 J and above form stable suspensions.

Figure 5 shows the scanning electron microscopy (SEM) micrographs of the buckypapers obtained before and after plasma treatment. Figure 5a shows that BPs without plasma treatment are well dispersed, and the nanotubes show no signs of defects. Hence, this result together with the characterization of the suspensions described above allows us to conclude that the energy used in the sonication process was sufficient to produce high-quality buckypapers, since there was no damage to the CNTs and they remained efficiently dispersed. However, after 1 minute of plasma treatment (Figure 5 b) the nanotubes are homogeneously coated with a layer that matches their tubular geometry. As the treatment time increases (Figures 5c, d) the thickness of the coating

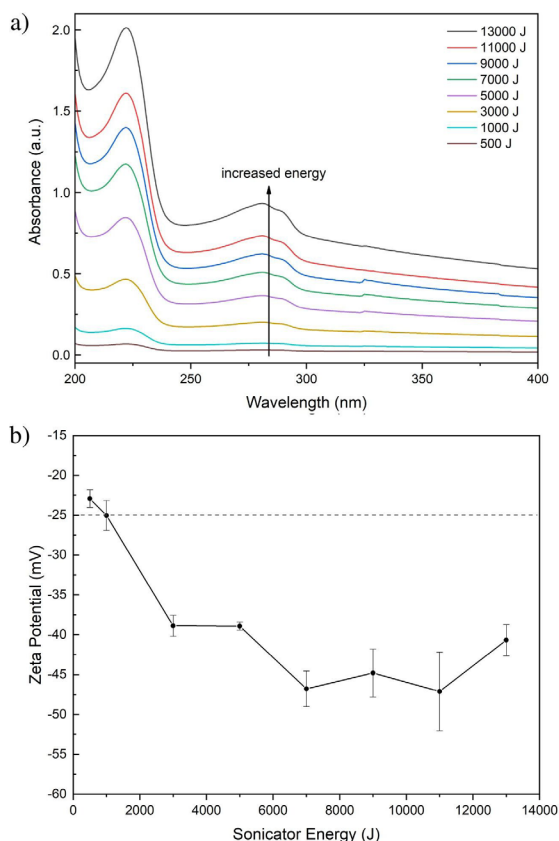


Figure 4. Absorption spectra (a) and Zeta potential (b) of MWCNT water dispersions produced with different sonication energies with 0.5 wt.% of Triton X-100 surfactant.

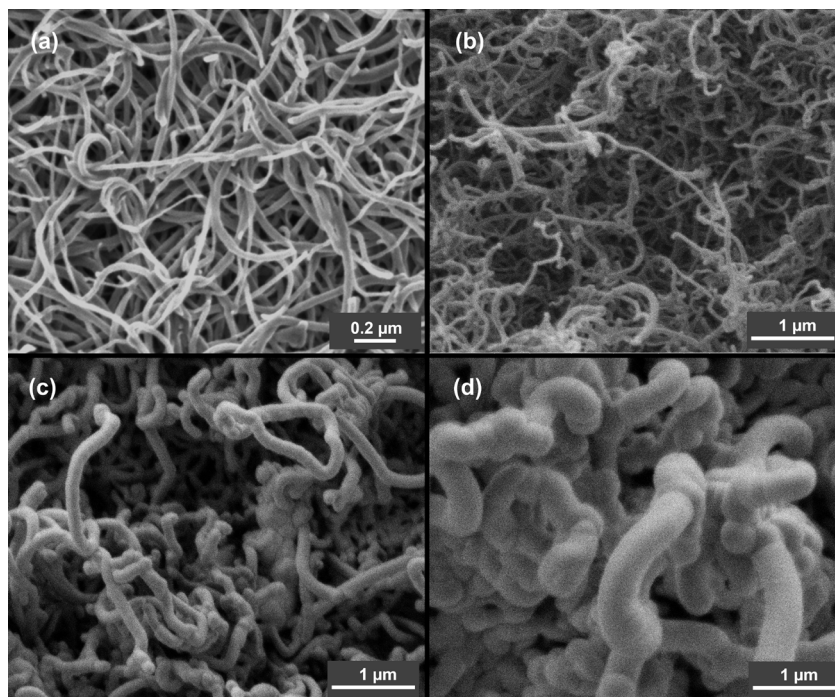


Figure 5. SEM micrographs of buckypapers: as prepared (a), after 1 (b), 3 (c) and 10 (d) minutes of plasma treatment with tetrafluoroethane.

layer increases, but no physical damage was observed on the nanotubes. By measuring the increasing thickness of the coated nanotubes as a function of the treatment time, an average deposition rate of 50 nm/min was determined.

A typical FTIR spectrum (Figure 6) of a fluorocarbon film shows three major peaks associated with amorphous plasma-polymerized fluorocarbon materials³⁵. One peak at 614 cm^{-1} corresponds to CF_2 wagging vibration, and a second broad and very prominent peak at $900\text{--}1400\text{ cm}^{-1}$ corresponds to all CF_x ($x = 1, 2 \text{ \& } 3$) stretching modes, which is characteristic of a cross-linked structure due to the intense presence of CF groups. Finally, the weak absorbance band at $1600\text{--}1730\text{ cm}^{-1}$ is attributed to unsaturated stretching modes of $\text{C}=\text{CF}_2$ and $\text{CF}=\text{CF}_2$ groups in the film. These bands result from the fluorine substitution of hydrogen on $\text{C}=\text{CH}_2$ bonds^{35,42-45}.

CF_2 and CF_3 radicals are largely responsible for the hydrophobic characteristics of polymeric materials, thus the presence of these radicals in films has a direct influence on their hydrophobic properties. Infrared spectra of polymeric materials, such as polytetrafluoroethylene, have intense and well-defined peaks referring to vibrational modes of CF_2 bonds at 1200 and 1100 cm^{-1} ⁴⁶. This pattern can also be seen in spectra of the 1,1,1,2 tetrafluoroethane gas, in which two main peaks of the radicals present in the gas phase are seen, C-H bonds in the range of 2900 cm^{-1} to 3000 cm^{-1} and the CF_2 monomer at 1100 cm^{-1} , previously reported by R. Labelle et. al.⁴⁷. In PECVD deposition, various radicals can be formed as the gas bonds are broken. There is a relationship between rf-power increase and bond breaking, giving rise to different radicals⁴⁸. As the bond-breaking intensifies, the formation of cross-links in the film structure increases, so a broadening of the peak at 1200 cm^{-1} occurs, due to vibrational modes of the bonds of the various radicals CF , CF_2 , and CF_3 .

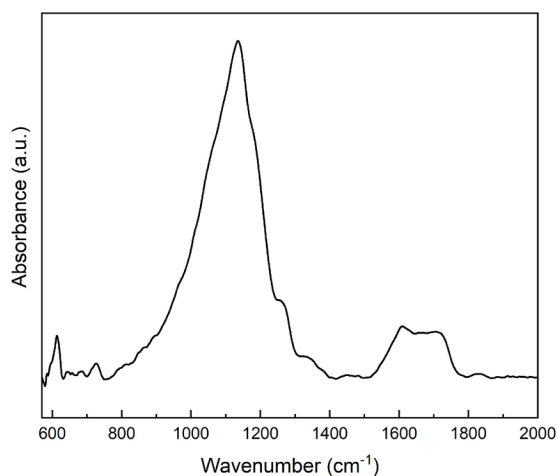


Figure 6. FTIR absorption of a fluorocarbon coating deposited on Si substrate.

XPS survey analysis (Figure 7) showed a composition of 48.08% total fluorine, 46.9% total carbon and 5.23% of oxygen (which is probably due to atmospheric contamination)⁴⁹⁻⁵¹, confirming the high fluorine content of the coatings. The high-resolution C1s spectrum (Figure 7) confirmed the presence of C-C (or C-CH), C-CF, CF, CF_2 and CF_3 groups centered at 284.6, 285.9, 287.8, 290.2 and 292.7 eV, respectively^{42,48,52,53}. The measured contact angle of a smooth Si surface coated with such fluorocarbon film was 120° ^{54,55}, confirming the high hydrophobicity of the coating. A more detailed analysis of the structure of these films will be presented in a separate publication.

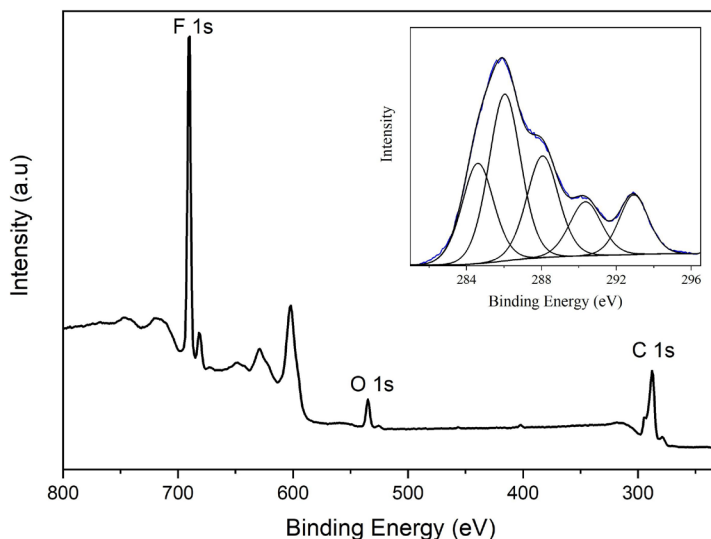


Figure 7. XPS spectra of a fluorocarbon coating deposited on Si substrate. The insert shows the C 1s high resolution spectrum.

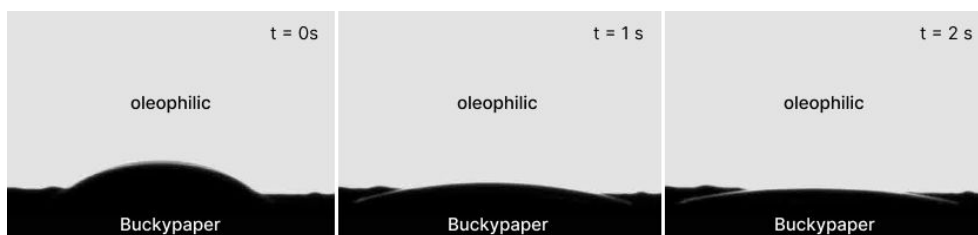


Figure 8. Photographic images of the absorption of an oil drop placed on top of a BP after plasma treatment for 10 minutes.

Contact angle measurements performed on samples without plasma treatment showed the hydrophilicity of the buckypaper. A drop of water placed on the buckypaper surface was quickly absorbed due to its porous structure. The same happened to the mineral oil for every treatment time (1, 3 and 10 minutes), meaning that the buckypaper was also oleophilic. Nevertheless, an initial contact angle of $36^\circ \pm 1^\circ$ could be estimated, as seen in Figure 8. Such behavior can be attributed to the high dispersion quality of CNTs and the material porosity. The empty spaces among the individual nanotubes favor the water and oil to flow inside the pores and to be absorbed.

To assess the influence of the plasma treatment time, contact angle measurements were performed on the buckypapers treated for 1, 3 and 10 minutes. Figure 9 shows that in all three cases the contact angles are compatible with superhydrophobic characteristics. The contact angle values were $145^\circ \pm 1^\circ$, $149^\circ \pm 1^\circ$ and $149^\circ \pm 1^\circ$ for 1, 3 and 10 minutes, respectively.

The contact angle results can be directly related to the combination of a decrease in the surface energy and the micro/nanostructured surface of the BPs. After the plasma treatment, the coated nanotubes get thicker and a nano/micro-textured surface with reduced pore sizes results. In addition to that, the surface energy decreases as the surface of CNTs is covered by a highly hydrophobic fluorocarbon film. As already

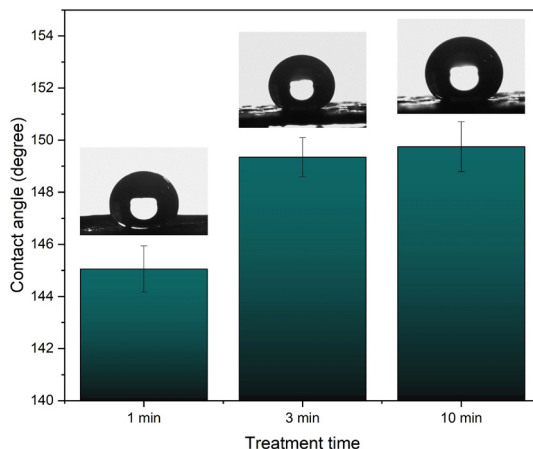


Figure 9. Water contact angle values for plasma treatment times of 1, 3 and 10 minutes. The insert shows the photographs of the water drops on the surface of the plasma-treated BPs.

mentioned, CF_2 and CF_3 radicals are mainly responsible for the hydrophobicity of fluorocarbon materials^{44,56-59}.

It was also observed that the water drops roll off easily over the surface, even for inclinations below 10 degrees. This fact, together with the high contact angle value obtained can be

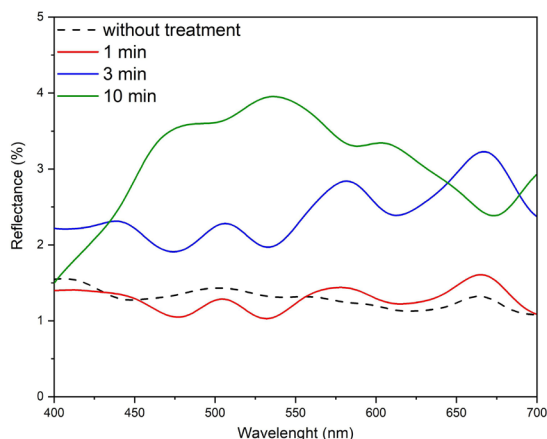


Figure 10. Optical reflectance of buckypapers as a function of wavelength in the range of visible light (400 to 700 nm).

attributed to air imprisoned in the porous surface of the sample, as explained by the Cassie-Baxter model. On the other hand, measurements performed with mineral oil showed that plasma-treated BPs remained oleophilic as the oil permeates completely through samples, regardless of the plasma treatment time.

The reflectance spectra in the visible light range obtained for the samples before and after plasma treatment are shown in Figure 10. The uncoated buckypaper showed an average reflectance of 1.30%, while the samples submitted to 1, 3 and 10 minutes of plasma coating presented reflectance of 1.30%, 2.31% and 3.29%, respectively. The very low reflectance of BP in the visible spectrum in the range of 1.1 to 1.5%, makes them potential candidates to be used in optical devices for various applications, including space applications. The BP submitted to 1-minute plasma coating did not show any significant reflectance changes compared to the uncoated BP and, thus, the average reflectance value in the 400 – 700 nm range remained essentially the same. However, longer treatment times of 3 and 10 minutes resulted in some increase in reflectance. The reflectance of the sample coated for 3 minutes showed a higher reflectance than the 1-minute sample while keeping the same overall pattern. This strongly indicates that the fluorocarbon film is becoming thicker by showing both the same characteristics of the 1-minute coated sample but with increasing values of reflectance. The higher reflectance values of the 10-minute coated sample caused by the much thicker coating (see Figure 5d), shifted the appearance of the samples from very dark black to dark green, with the highest values of reflectance around 530 nm, which corresponds to the green color in the visible light spectrum. BPs after 1 and 3 minutes of plasma treatment showed no change at all in their colors. All the observed spectra behave similarly, presenting slight oscillations (~0.5% amplitude) which cannot be attributed to the apparatus, as confirmed by careful calibration of the measurements with a sapphire sample. This effect is thought to be due to interference effects inside the samples.

4. Conclusions

An effective method of producing BPs with superhydrophobic/oleophilic properties was presented by

means of plasma treatment with 1, 1, 1, 2 tetrafluoroethane ($C_2H_2F_4$). Superhydrophobic/oleophilic properties were obtained after 1 min of plasma treatment, demonstrating a fast and inexpensive method of producing buckypapers with these wettability properties. Water contact angles greater than 140° were obtained and these results are attributed to the combination of the modification of surface micro/nanostructures and the reduction of surface energy due to the coating with a fluorocarbon film. BPs also showed very low optical reflectance values in the visible light range, reaching an average value of approximately 1.30%, outperforming many commercial materials. The low optical reflectance remained essentially unchanged when a 1-minute plasma treatment was employed. The results obtained suggest that a good combination of low reflectance and superhydrophobic/oleophilic behavior can be achieved by a good dispersion of CNTs and fluorocarbon coating. This is of potential importance for technology applications that require super black surfaces while preventing water from penetrating or being absorbed by the surface, improving the handling of optical signals and extending the life of materials.

5. Acknowledgments

The authors gratefully acknowledge the CTNano – Universidade Federal de Minas Gerais for supplying the carbon nanotubes used in this work, the Van de Graaff Laboratory of PUC-Rio for the XPS analysis and FAPERJ for financial support.

6. References

- Du C, Zhao H, Dai Z, Tian Z, Wang J, Wang Z. The preparation and properties of black coating by micro arc oxidation on 2A12 aluminum alloy. *Mater Lett.* 2019;236:723-6.
- Surrey NanoSystems. About Vantablack [Internet]. 2022 [cited 2022 Jul 14]. Available from: <https://www.surreynanosystems.com/about/vantablack>
- Azoubel S, Cohen R, Magdassi S. Wet deposition of carbon nanotube black coatings for stray light reduction in optical systems. *Surf Coat Tech.* 2015;262:21-5.
- Chen JZ, Wang C, Hsu CC, Cheng IC. Ultrafast synthesis of carbon-nanotube counter electrodes for dye-sensitized solar cells using an atmospheric-pressure plasma jet. *Carbon.* 2016;98:34-40.
- Bera RK, Binyamin Y, Frantz C, Uhlig R, Magdassi S, Mandler D. Fabrication of self-cleaning CNT-based near-perfect solar absorber coating for non-evacuated concentrated solar power applications. *Energy Technol.* 2020;8(12):2000699.
- Saji VS. Carbon nanostructure-based superhydrophobic surfaces and coatings. *Nanotechnol Rev.* 2021;10(1):518-71.
- Tobias G, Mendoza E, Ballesteros B. Functionalization of carbon nanotubes. In: Bhushan B, editor. *Encyclopedia of nanotechnology.* Dordrecht: Springer Netherlands; 2016. p. 1281-91. http://dx.doi.org/10.1007/978-94-017-9780-1_48.
- Meyyappan M, editor. *Carbon nanotubes.* Boca Raton: CRC Press; 2004. <http://dx.doi.org/10.1201/9780203494936>.
- Iijima S. Helical microtubules of graphitic carbon. *Nature.* 1991;354(6348):56-8.
- Ji X, Li X, Yu H, Zhang W, Dong H. Study on the carbon nanotubes reinforced nanocomposite coatings. *Diamond Relat Mater.* 2019;91:247-54.
- Han T, Nag A, Chandra Mukhopadhyay S, Xu Y. Carbon nanotubes and its gas-sensing applications: a review. *Sens Actuators Phys.* 2019;291:107-43.

12. Campos RBV, Camargo SAS Jr, Brum MC, Santos DS. Hydrogen uptake enhancement by the use of a magnesium hydride and carbon nanotubes mixture. *Mater Res*. 2017;20(Suppl. 1):85-8.
13. Lv S, Ma L, Shen X, Tong H. Potassium chloride-catalyzed growth of porous carbon nanotubes for high-performance supercapacitors. *J Alloys Compd*. 2022;906:164242.
14. Sawant SV, Patwardhan AW, Joshi JB, Dasgupta K. Boron doped carbon nanotubes: synthesis, characterization and emerging applications: a review. *Chem Eng J*. 2022;427:131616.
15. Hammar A, Christensen OM, Park W, Pak S, Emrich A, Stake J. Stray light suppression of a compact off-axis telescope for a satellite-borne instrument for atmospheric research. In: Wang Y, Tatsuno K, Kidger TE, editors. *Optical design and testing VIII*. Beijing: SPIE; 2018. p. 15. <http://dx.doi.org/10.1117/12.2500555>.
16. Sreekumar TV, Liu T, Kumar S, Ericson LM, Hauge RH, Smalley RE. Single-wall carbon nanotube films. *Chem Mater*. 2003;15(1):175-8.
17. Dumée LF, Sears K, Schütz J, Finn N, Huynh C, Hawkins S, et al. Characterization and evaluation of carbon nanotube Bucky-Paper membranes for direct contact membrane distillation. *J Membr Sci*. 2010;351(1-2):36-43.
18. Abreu B, Pires AS, Guimarães A, Fernandes RMF, Oliveira IS, Marques EF. Polymer/surfactant mixtures as dispersants and non-covalent functionalization agents of multiwalled carbon nanotubes: synergism, morphological characterization and molecular picture. *J Mol Liq*. 2022;347:118338.
19. Coleman JN, Khan U, Gun'ko YK. Mechanical reinforcement of polymers using carbon nanotubes. *Adv Mater*. 2006;18(6):689-706.
20. Kharisova OV, Kharisov BI, Casas Ortiz EG. Dispersion of carbon nanotubes in water and non-aqueous solvents. *RSC Advances*. 2013;3(47):24812.
21. Sezer N, Koç M. Stabilization of the aqueous dispersion of carbon nanotubes using different approaches. *Therm Sci Eng Prog*. 2018;8:411-7.
22. Bao HD, Sun Y, Xiong ZY, Guo ZX, Yu J. Effects of the dispersion state and aspect ratio of carbon nanotubes on their electrical percolation threshold in a polymer. *J Appl Polym Sci*. 2013;128(1):735-40.
23. Fatemi SM, Foroutan M. Recent developments concerning the dispersion of carbon nanotubes in surfactant/polymer systems by MD simulation. *J Nanostructure Chem*. 2016;6(1):29-40.
24. Thostenson ET, Ren Z, Chou TW. Advances in the science and technology of carbon nanotubes and their composites: a review. *Compos Sci Technol*. 2001;61(13):1899-912.
25. Borovskaya AO, Idiatullin BZ, Zueva OS. Carbon nanotubes in the surfactants dispersion: formation of the microenvironment. *J Phys Conf Ser*. 2016;690:012030.
26. Duan WH, Wang Q, Collins F. Dispersion of carbon nanotubes with SDS surfactants: a study from a binding energy perspective. *Chem Sci*. 2011;2(7):1407.
27. Tan Y, Resasco DE. Dispersion of single-walled carbon nanotubes of narrow diameter distribution. *J Phys Chem B*. 2005;109(30):14454-60.
28. Kim SW, Kim T, Kim YS, Choi HS, Lim HJ, Yang SJ, et al. Surface modifications for the effective dispersion of carbon nanotubes in solvents and polymers. *Carbon*. 2012;50(1):3-33.
29. Rojas JA, Ardila-Rodríguez LA, Diniz MF, Gonçalves M, Ribeiro B, Rezende MC. Optimization of Triton X-100 removal and ultrasound probe parameters in the preparation of multiwalled carbon nanotube buckypaper. *Mater Des*. 2019;166:107612.
30. Ma PC, Mo SY, Tang BZ, Kim JK. Dispersion, interfacial interaction and re-agglomeration of functionalized carbon nanotubes in epoxy composites. *Carbon*. 2010;48(6):1824-34.
31. Strano MS, Dyke CA, Usrey ML, Barone PW, Allen MJ, Shan H, et al. Electronic structure control of single-walled carbon nanotube functionalization. *Science*. 2003;301(5639):1519-22.
32. Haynes WM, Lide DR, editors. *CRC handbook of chemistry and physics: a ready-reference book of chemical and physical data*. 96th ed. Boca Raton: CRC Press; 2015.
33. Yang S, Xia Q, Zhu L, Xue J, Wang Q, Chen Q. Research on the icephobic properties of fluoropolymer-based materials. *Appl Surf Sci*. 2011;257(11):4956-62.
34. Antonietti M, Henke S, Thünemann A. Highly ordered materials with ultra-low surface energies: Polyelectrolyte-surfactant, complexes with fluorinated surfactants. *Adv Mater*. 1996;8(1):41-5.
35. Brown PS, Bhushan B. Bioinspired, roughness-induced, water and oil super-philic and super-phobic coatings prepared by adaptable layer-by-layer technique. *Sci Rep*. 2015;5(1):14030.
36. Wang Z, Liang Z, Wang B, Zhang C, Kramer L. Processing and property investigation of single-walled carbon nanotube (SWNT) buckypaper/epoxy resin matrix nanocomposites. *Compos Part Appl Sci Manuf*. 2004;35(10):1225-32.
37. Han JH, Zhang H, Chen MJ, Wang GR, Zhang Z. CNT buckypaper/thermoplastic polyurethane composites with enhanced stiffness, strength and toughness. *Compos Sci Technol*. 2014;103:63-71.
38. Zhang Z, Wei H, Liu Y, Leng J. Self-sensing properties of smart composite based on embedded buckypaper layer. *Struct Health Monit*. 2015;14(2):127-36.
39. Dai W, Wang D. Cutting methods and perspectives of carbon nanotubes. *J Phys Chem C*. 2021;125(18):9593-617.
40. Grossiord N, Regev O, Loos J, Meuldijk J, Koning CE. Time-dependent study of the exfoliation process of carbon nanotubes in aqueous dispersions by using UV-visible spectroscopy. *Anal Chem*. 2005;77(16):5135-9.
41. Rausch J, Zhuang RC, Mäder E. Surfactant assisted dispersion of functionalized multi-walled carbon nanotubes in aqueous media. *Compos Part Appl Sci Manuf*. 2010;41(9):1038-46.
42. Butoi CI, Mackie NM, Gamble LJ, Castner DG, Bamd J, Miller AM, et al. Deposition of highly ordered CF₂-rich films using continuous wave and pulsed hexafluoropropylene oxide plasmas. *Chem Mater*. 2000;12(7):2014-24.
43. Shiomi H. Reactive ion etching of diamond in O₂ and CF₄ plasma, and fabrication of porous diamond for field emitter cathodes. *Jpn J Appl Phys*. 1997;36(Part 1, No. 12B):7745-8.
44. Zhang L, Wang F, Qiang L, Gao K, Zhang B, Zhang J. Recent advances in the mechanical and tribological properties of fluorine-containing DLC films. *RSC Advances*. 2015;5(13):9635-49.
45. Capps NE, Mackie NM, Fisher ER. Surface interactions of CF₂ radicals during deposition of amorphous fluorocarbon films from CHF₃ plasmas. *J Appl Phys*. 1998;84(9):4736-43.
46. Piwowarczyk J, Jędrzejewski R, Moszyński D, Kwiatkowski K, Niemczyk A, Baranowska J. XPS and FTIR studies of polytetrafluoroethylene thin films obtained by physical methods. *Polymers*. 2019;11(10):1629.
47. Labelle CB, Karecki SM, Reif R, Gleason KK. Fourier transform infrared spectroscopy of effluents from pulsed plasmas of 1,1,2,2-tetrafluoroethane, hexafluoropropylene oxide, and difluoromethane. *J Vac Sci Technol Vac Surf Films*. 1999;17(6):3419-28.
48. Wang YR, Ma WC, Lin JH, Lin HH, Tsai CY, Huang C. Deposition of fluorocarbon film with 1,1,1,2-tetrafluoroethane pulsed plasma polymerization. *Thin Solid Films*. 2014;570:445-50.
49. Lappan U, Geißler U, Lunkwitz K. Changes in the chemical structure of polytetrafluoroethylene induced by electron beam irradiation in the molten state. *Radiat Phys Chem*. 2000;59(3):317-22.
50. Lau KKS, Caulfield JA, Gleason KK. Structure and morphology of fluorocarbon films grown by hot filament chemical vapor deposition. *Chem Mater*. 2000;12(10):3032-7.
51. Quade A, Polak M, Schröder K, Ohla A, Weltmann KD. Formation of PTFE-like films in CF₄ microwave plasmas. *Thin Solid Films*. 2010;518(17):4835-9.
52. Golub MA, Wydeven T, Cormia RD. Plasma copolymerization of ethylene and tetrafluoroethylene. *J Polym Sci Part Polym Chem*. 1992;30(13):2683-92.

53. da Costa MEHM, Freire FL Jr. Surface modifications of amorphous hydrogenated carbon films submitted to carbon tetrafluorine plasma treatment. *Diamond Relat Mater.* 2012;22:1-5.
54. Yu S, Wang X, Wang W, Yao Q, Xu J, Xiong W. A new method for preparing bionic multi scale superhydrophobic functional surface on X70 pipeline steel. *Appl Surf Sci.* 2013;271:149-55.
55. Shafrin EG, Zisman WA. Upper limits for the contact angles of liquids on solids. Washington: Naval Research Laboratory; 1963.
56. Bendavid A, Martin PJ, Randeniya L, Amin MS. The properties of fluorine containing diamond-like carbon films prepared by plasma-enhanced chemical vapour deposition. *Diamond Relat Mater.* 2009;18(1):66-71.
57. Butter RS, Waterman DR, Lettington AH, Ramos RT, Fordham EJ. Production and wetting properties of fluorinated diamond-like carbon coatings. *Thin Solid Films.* 1997;311(1-2):107-13.
58. Yao ZQ, Yang P, Huang N, Sun H, Wang J. Structural, mechanical and hydrophobic properties of fluorine-doped diamond-like carbon films synthesized by plasma immersion ion implantation and deposition (PIII-D). *Appl Surf Sci.* 2004;230(1-4):172-8.
59. Yu GQ, Tay BK, Sun Z, Pan LK. Properties of fluorinated amorphous diamond like carbon films by PECVD. *Appl Surf Sci.* 2003;219(3-4):228-37.